

Supporting Information

Grafting silicone at room temperature – a transparent, scratch-resistant non-stick molecular coating

Hannu Teisala, Philipp Baumli, Stefan A. L. Weber, Doris Vollmer* and Hans-Jürgen Butt*

Contents:

- 1. Supplementary Discussion**
- 2. Supplementary Figures**
- 3. Supplementary Tables**
- 4. Supplementary Videos**
- 5. Supplementary References**

1. Supplementary Discussion

Characterizing wetting of surfaces by water

Surface water repellency is commonly characterized by measuring static contact angles θ after a water drop is deposited on a surface or by measuring advancing contact angles θ_a and receding contact angles θ_r when the water drop is inflated or deflated. The difference between θ_a and θ_r is termed contact angle hysteresis. It describes the adhesion force of the drop to the surface¹⁻³. Additionally, sliding angle or roll-off angle, *i.e.* the angle at which a drop of certain size starts to move when the substrate is inclined, is used to characterize the wetting properties of surfaces. High receding contact angle and low sliding angle are required to shed drops easily and to keep surfaces clean.

Sliding drops

Hydrophobicity alone is not a sufficient condition to induce self-cleaning of a surface. Shedding of liquids, leaving the surface dry, is crucial. Otherwise, particle contamination on the surface cannot be collected by drops or contaminants from evaporating drops are left on the surface (Figure 1a and Video S2).

Both the velocity and the contact angle hysteresis of sliding water drops depend on the inclination angle of the sample (Table S2). At an inclination of 15° of a PDMS grafted glass surface, the drop velocity is about 10 $\mu\text{m s}^{-1}$ and the contact angle hysteresis measured from the moving drops was only $4 \pm 1^\circ$ (Figure S3). On the same sample surface, at an inclination of 45°, the drop velocity was of the order of 2.6 mm s^{-1} , and the contact angle hysteresis increased to 15°. That is, θ_a and θ_r are not absolute values but are dependent on the velocity of the moving three-phase contact lines in the front and the rear of the drop, respectively⁴⁻⁷.

Organic liquids start to slide on the PDMS films much more easily than water. Typically, 10 μL drops start to slide at inclinations even below 5° (Figure 1f). In addition, the sliding velocity generally is much faster as compared to that of water. Already at inclinations below 10°, the sliding velocity of organic liquids is typically of the order of mm s^{-1} .

Light transmittance

The PDMS films are 100% transparent as verified by UV-Vis spectroscopy (Figure S4). This is due to the small refractive index mismatch, only about 3%, between PDMS and silicon oxide and because the coating film is only a few nm thick and does not contain any light reflecting surface structures which hinder light transmission.

Coating different substrates

Additionally to the borosilicate glass substrate used in the experiments, we grafted PDMS MW 6 000 g mol⁻¹ to soda-lime laboratory glass and a glass vial (Video S5). After applying a thin silica layer (~3 nm thick) onto the substrate surface by the gas-phase Stöber-like reaction, we managed to PDMS-coat aluminum and stainless steel plates, and porous surfaces of polyester fabric and paper, Figure S5, Table S3, and Video S3.

PDMS films as anti-icing coatings

The PDMS films significantly reduce ice adhesion on glass. On the PDMS coated glass, ice adhesion strength was only 2.7±0.6 kPa, whereas on uncoated, clean glass surface the ice adhesion strength was 155±17 kPa. That is, the PDMS coating reduced the ice adhesion by more than 98% as compared to the uncoated glass surface.

Freezing of 50 µL drops that were used in the experiments takes only a few minutes. Therefore, with our ice adhesion measurement setup full ice adhesion is reached already after freezing time of 10 min. With large ice blocks that are typically used in ice adhesion measurements, freezing times of several hours (overnight) are required. Another advantage of the small drop size is that several independent measurements can be carried out on a small sample area (Figure S6). Therefore, our setup allows fast and repeated ice adhesion strength measurements. We measured ice adhesion strength on the PDMS coated glass repeatedly 20 times on 5 individual spots. We marked target positions for the drops underneath the glass sample so that the drops could be placed at the same location each time. Within the 20 experiments, the ice adhesion strength remained unchanged within the experimental accuracy (Figure 3b, inset).

In addition, we measured ice adhesion on some other, commonly used materials to verify our results with the results obtained by other groups with different ice adhesion measurement setups. We measured ice adhesion of 152±48 kPa on Teflon (PTFE), 104±25 kPa on cross-linked PDMS, 657±49 kPa on aluminum, and 235±34 kPa on stainless steel. The ice adhesion strength values measured on the reference materials in this work are of the same order of magnitude that other researchers have reported previously, Table S4⁸⁻¹⁷.

FTIR monitoring of PDMS reactions at silicon oxide surface

We monitored the room temperature grafting reaction of PDMS *in-situ* by FTIR (Figures 8 and S7). To maximize the surface area for the reaction, we contacted PDMS (MW 6 000 g mol⁻¹) with densely packed silicon dioxide particles (surface area = 200 m² g⁻¹). Evolution of the whole spectrum after contacting PDMS with the particles is shown in Figure 8a and magnification of the absorption bands from hydroxyl groups and water at 3 000–4 000 cm⁻¹ in Figure 8b. Magnifications of the characteristic bands for PDMS¹⁸ and silicon dioxide¹⁹ are shown in Figure 8c–d. At the beginning of the reaction, the bands from the methyl groups (Si–CH₃) and the siloxane backbone (Si–O–Si) of PDMS reduce. These changes are associated with the hydrolysis of PDMS by the physisorbed water at the silicon dioxide surface, *i.e.* the regular structure of PDMS chains

containing the methyl groups and siloxane bonds, $-\text{Si}(\text{CH}_3)_2-\text{O}-\text{Si}(\text{CH}_3)_2-$, is converted to hydroxyl terminated chains, $-\text{Si}(\text{CH}_3)_2-\text{OH}$. When the reaction proceeds, both the bands from the siloxane bonds and the methyl groups start to increase, indicating growth of attached PDMS chains *via* condensation of hydrolyzed PDMS. Notably, the increment in the signal from the siloxane bonds and the methyl groups during the grafting process does not arise solely from establishing new siloxane bonds while grafting the PDMS chains, but the replacement of the initial physisorbed water layer at the silicon dioxide surface also contributes to the increased signal.

It is possible that the changes shown by the FTIR spectra are also partially caused by capillary driven rearrangements within the particle–PDMS fluid system during the experiment. In addition, we cannot exclude that some air remained trapped between the particles. Nevertheless, the differences in the relative changes of the bands from the siloxane bonds and the methyl groups indicate chemical changes in PDMS, which are associated with the hydrolysis and condensation reactions during the room temperature grafting of PDMS on silicon oxide. For example, after 24 h of grafting the band from siloxane bonds still slightly increased (Figure 8c) while the bands from the methyl groups remained unchanged or even decreased. FTIR spectra for the neat PDMS fluid and the neat silicon dioxide particles are shown in Figures S7a and S7b, respectively.

Large-scale application of PDMS films

The PDMS films can be applied using well-established coating techniques suitable for large-scale production. To demonstrate the easy applicability of the coatings, we used a multitude of different approaches to deposit the coatings including painting, spraying, and roll-coating (Video S4). In large-scale production, it is desirable to avoid using solvents in all steps of the coating procedure. Therefore, we tested producing PDMS films without using any solvents, even in the washing step. After letting PDMS MW 6 000 g mol^{-1} react with the glass substrate for 24 h at room temperature, we simply polished the surface with a paper tissue so that all visible PDMS was removed (Video S4). After polishing, a tiny amount of unbound lubricating PDMS remains on the surface held in place by the grafted PDMS chains. Although the free PDMS can still continue reacting with the grafted PDMS, the anti-wetting properties of the film remained good after 1 month storing in laboratory air, *i.e.* contact angle hysteresis of water was $12\pm 2^\circ$ and the sliding angle for 10 μL water drops was $7\pm 2^\circ$.

2. Supplementary Figures

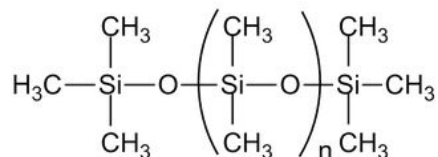


Figure S1. Molecular formula of trimethylsiloxy terminated linear polydimethylsiloxane (PDMS).

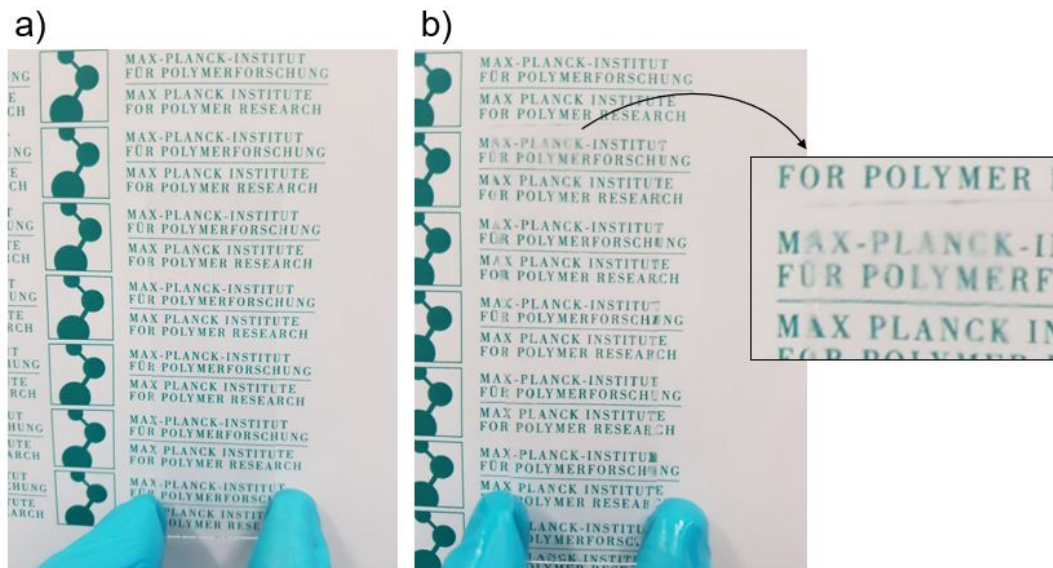


Figure S2. Unmodified and PDMS modified glass after insufficient rinsing. a) Undisturbed view to printed letters below an unmodified glass. b) Blurry view due to unbound, thick layer of PDMS remaining on glass after insufficient rinsing in solvents. The sample was rinsed in toluene, ethanol, and water for 10 s in each liquid.

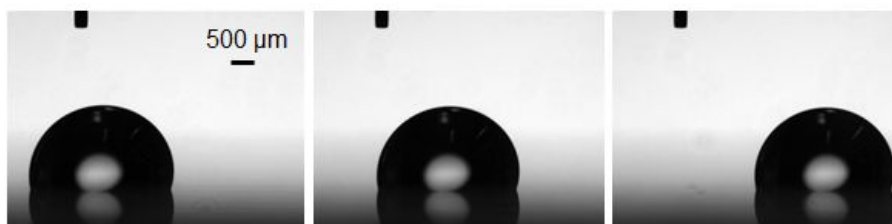


Figure S3. Water drop (10 μL) sliding down on a PDMS film grafted to glass at room temperature for 24 h. The sample was inclined by 15° , and the drop had a velocity of $10 \mu\text{m s}^{-1}$. Contact angle hysteresis, *i.e.* the difference between θ_a in the front and θ_r in the rear of the drop, respectively, is 4° . PDMS molecular weight was $6\,000 \text{ g mol}^{-1}$.

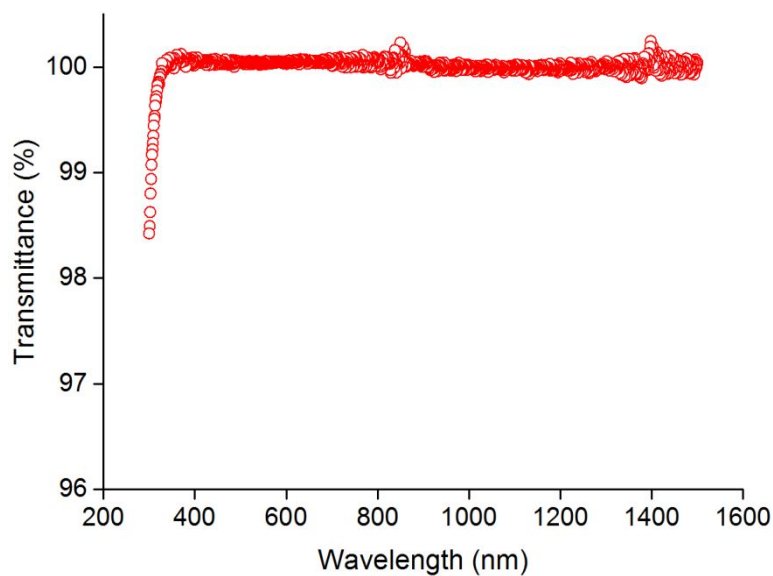


Figure S4. Light transmittance of PDMS film grafted to glass at room temperature for 24 h. PDMS molecular weight was $6\,000\text{ g mol}^{-1}$. Light transmittance is normalized to the transmittance of the uncoated glass substrate.

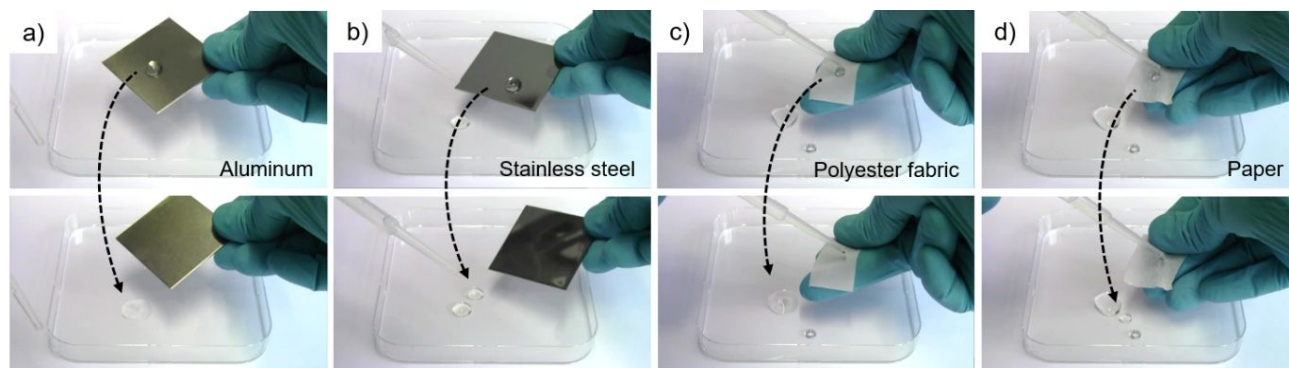


Figure S5. Water repellent PDMS films grafted to silica modified substrates. a) Aluminum, b) stainless steel, c) polyester fabric, and d) paper tissue grafted with PDMS at room temperature for 24 h. PDMS molecular weight was $6\,000\text{ g mol}^{-1}$.

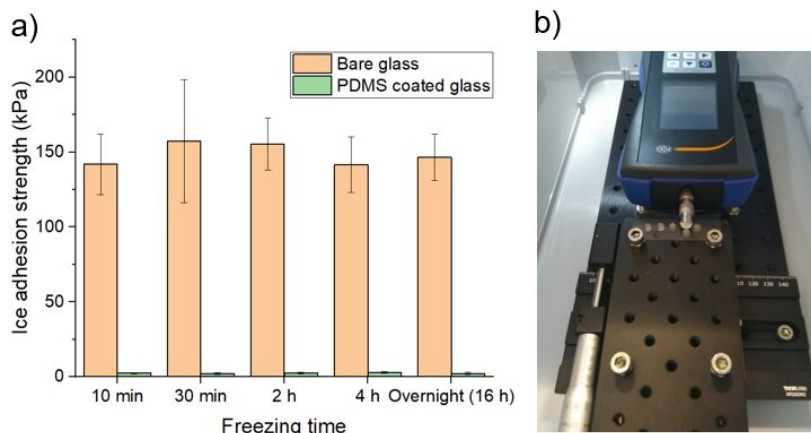


Figure S6. Characteristics of the home-built ice adhesion measurement device. The whole setup is built in a portable cooling chamber. The temperature inside the chamber remains at -8°C during the measurements. Drop size and wettability of the sample surface, *i.e.* the static contact angle, decide the drop/sample contact area. Therefore, the contact area for the $50\ \mu\text{L}$ drop size that was used in the experiments was determined for each sample material independently prior to the force measurements. a) Ice adhesion strength with varying freezing time measured on uncoated glass and on PDMS films grafted to glass. Full ice adhesion strength on both sample materials is achieved already after 10 min of freezing. b) A photograph of the ice adhesion measurement setup. The small drop size allows rapid freezing and multiple parallel measurements on a small sample area. The PDMS films were grafted at room temperature for 24 h. PDMS molecular weight was $6\ 000\ \text{g mol}^{-1}$.

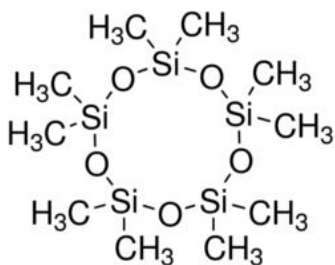


Figure S7. Molecular formula of decamethylcyclopentasiloxane (D5).

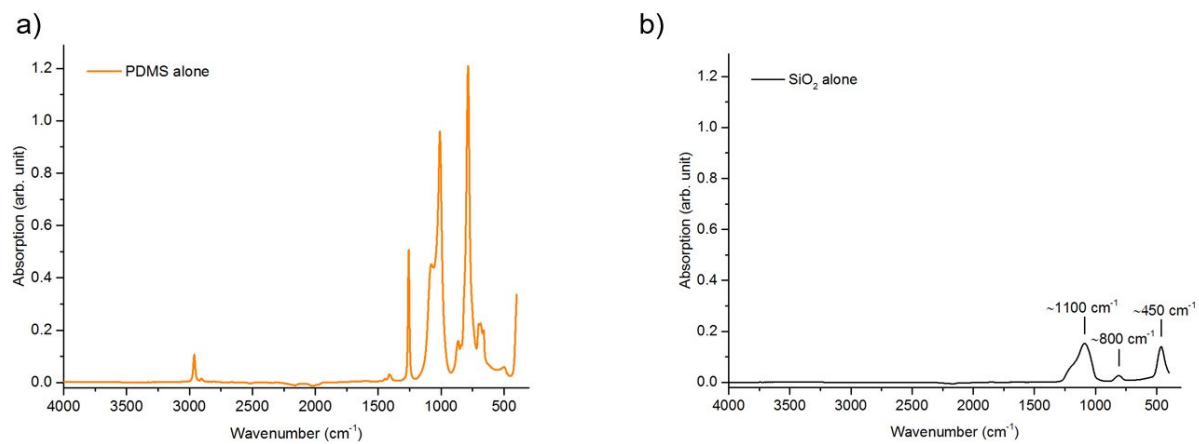


Figure S8. Absorption spectra from a) neat PDMS fluid and b) neat silicon dioxide particles.

3. Supplementary Tables

Table S1. Physicochemical properties of Si-X and C-X bonds²⁰.

Element [X]	Bond length [Å]		Ionic character [%]	
	Si-X	C-X	Si-X	C-X
Si	2.34	1.88	-	12
C	1.88	1.54	12	-
H	1.47	1.07	2	4
O	1.63	1.42	50	22

Table S2. Contact angle hysteresis for 10 μ L water drops sliding down on a PDMS film grafted to glass at room temperature for 24 h. Drop velocity and contact angle hysteresis increase with increasing tilt angle of the substrate. PDMS molecular weight was 6 000 g mol⁻¹.

Tilt angle [°]	Velocity [μ m s ⁻¹]	θ_a [°]	θ_r [°]	$\theta_a - \theta_r$ [°]
15	10	107 \pm 1	103 \pm 1	4
30	600	107 \pm 1	99 \pm 1	8
45	2600	109 \pm 2	94 \pm 3	15

Table S3. Water repellency of PDMS films grafted to silica modified surfaces of aluminum, stainless steel, polyester fabric, and paper tissue at room temperature. PDMS molecular weight was 6 000 g mol⁻¹. Prior to the PDMS grafting, the aluminum and stainless steel plates showed water contact angle hysteresis of 104 \pm 3° and 54 \pm 2°, respectively. Before the grafting, the polyester fabric showed a static water contact angle θ of about 55°. However, θ continuously decreased as water spread within the surface structure *via* capillary wicking. Prior to the PDMS grafting, the paper tissue showed perfect wetting ($\theta = 0^\circ$) and absorption of water. Note, θ continuously decreased as water was sucked into the tissue *via* capillary wicking.

Grafting time [h]	Substrate	θ [°]	θ_a [°]	θ_r [°]	$\theta_a - \theta_r$ [°]	α [°]
24	Aluminum	113 \pm 1	116 \pm 4	89 \pm 3	27	-
24	Stainless steel	108 \pm 1	111 \pm 1	101 \pm 1	10	12 \pm 2
24	Polyester fabric	143 \pm 4	147 \pm 2	134 \pm 4	13	40 \pm 5
24	Paper tissue	124 \pm 10	-	-	-	-

Table S4. Wettability and ice adhesion strength on different test materials. In the present work aluminum, stainless steel, bare glass, and Teflon were cleaned with ethanol and water and dried under nitrogen flow prior to measurements. Ice adhesion strength was measured at -8°C . The PDMS films were grafted at room temperature for 24 h. PDMS molecular weight was $6\,000\text{ g mol}^{-1}$.

Material	θ [°]	θ_a [°]	θ_r [°]	$\theta_a - \theta_r$ [°]	Ice adh. strength [kPa]
Aluminum	97±3	104±3	0	104	657±49; 317±25 ¹⁵
Stainless steel	86±1	91±1	38±2	53	235±34; 172±17 ¹⁶
Bare glass	53±1	58±1	16±1	42	155±17
Teflon (PTFE)	105±1 ²¹	110±1 ²¹	78±2 ²¹	32 ²¹	152±48; 268±13 ²¹ ; 44±3 ¹²
Fluorosilane coating	119±1	126±1	85±3	41	124±13
Cross-linked PDMS	116±1	119±1	95±1	24	104±25
Superhydrophobic surface	163±2 ¹⁵	-	-	6 ¹⁵	65.4±18 ¹⁵
Slippery liquid-infused surface	-	117±3 ¹⁴	115±3 ¹⁴	2 ¹⁴	15.6±3.6 ¹⁴
Grafted PDMS on glass	106±1	109±1	97±1	12	2.7±0.6

Reference ice adhesion values from Refs^{15, 16, 21, 12, 14} were measured at the temperatures between -5°C and -10°C .

Table S5. Water repellency of PDMS films grafted to contaminated glass at room temperature for 1–24 h. The glass surface was not cleaned by oxygen plasma prior to the grafting. Thus, most of the surface silanols were occupied by atmospheric contaminants such as hydrocarbons. Therefore, the glass surface was less hydrophilic than plasma cleaned glass. PDMS molecular weight was $6\,000\text{ g mol}^{-1}$.

Grafting time [h]	θ [°]	θ_a [°]	θ_r [°]	$\theta_a - \theta_r$ [°]	α [°]
1	85±1	87±1	55±1	32	-
2	92±1	97±1	62±1	35	-
24	103±1	107±1	81±1	26	-

4. Supplementary Videos

Video S1. Flow of water drops over lubricant-infused cross-linked PDMS film and grafted PDMS film (24 h grafting at room temperature, the molecular weight of PDMS was 6 000 g mol⁻¹). The cross-linked PDMS (Sylgard 184) was infused with PDMS fluid of molecular weight of 6 000 g mol⁻¹. The surfaces were inclined by 30° and water drops, about 150 drops/min with a volume of 50 µL per drop, were continuously sliding over the samples.

Video S2. Colored water drop (radius ≈ 2 mm, the drop was dyed with methylene blue) sliding down on the PDMS coated glass. The drop leaves behind a clean surface. The sample was inclined by 15°, and the drop was released to the surface from the height of 1 cm. On a fluorosilane coated glass the drop pins and leaves behind a stain. PDMS was grafted at room temperature for 24 h. PDMS molecular weight was 6 000 g mol⁻¹.

Video S3. PDMS coatings on different substrates. The coated materials are silica modified aluminum, stainless steel, polyester fabric, and paper. PDMS was grafted at room temperature for 24 h. PDMS molecular weight was 6 000 g mol⁻¹. The liquid used to demonstrate repellency was water.

Video S4. Grafting PDMS to glass. PDMS can be applied to surfaces by well-established methods. After the grafting reaction, excess PDMS was removed from the substrate with a paper tissue. PDMS molecular weight was 6 000 g mol⁻¹. The liquids used to demonstrate repellency were water, ethanol, *n*-hexadecane, and diiodomethane.

Video S5. Different types of glass coated with PDMS films. The coatings were applied on a 170 µm thick borosilicate cover glass slide, a 1 mm thick soda-lime laboratory glass, and a glass vial. PDMS was grafted at room temperature for 24 h. PDMS molecular weight was 6 000 g mol⁻¹. The liquid used to demonstrate repellency was water.

Video S6. Mechanical stability of the PDMS coatings. The coated glass withstands polishing with a cleaning tissue, rubbing, abrasion, scratching, and repeated attachment and detachment of an adhesive tape. The substrate was 1 mm thick soda-lime laboratory glass. PDMS was grafted at room temperature for 24 h. PDMS molecular weight was 6 000 g mol⁻¹. The liquid used to demonstrate repellency was water.

Video S7. Abrading a superamphiphobic coating with a rubber glove. The liquid used to demonstrate repellency was water.

Videos S8. The PDMS coated glass repels super glue. PDMS was grafted at room temperature for 24 h. PDMS molecular weight was 6 000 g mol⁻¹. The liquid used to demonstrate repellency was water.

Video S9. The PDMS coated glass repels permanent markers and provides easy-to-clean properties. The substrate was 1 mm thick soda-lime laboratory glass. PDMS was grafted at room temperature for 24 h. PDMS molecular weight was 6 000 g mol⁻¹. The liquid used to demonstrate repellency was water.

Video S10. The PDMS coated glass shows dewetting of spray paint. The substrate was 1 mm thick soda-lime laboratory glass. PDMS was grafted at room temperature for 24 h. PDMS molecular weight was 6 000 g mol⁻¹.

5. Supplementary References

1. Marmur, A., Hydro- hygro- oleo- omni-phobic? Terminology of wettability classification. *Soft Matter* **2012**, 8 (26), 6867-6870.
2. Frenkel, Y. I., On the behavior of liquid drops on a solid surface. 1. The sliding of drops on an inclined surface. *J. Exptl. Theoret. Phys.* **1948**, 18, 658-667.
3. Gao, N.; Geyer, F.; Pilat, D. W.; Wooh, S.; Vollmer, D.; Butt, H.-J.; Berger, R., How drops start sliding over solid surfaces. *Nat. Phys.* **2018**, 14, 191-196.
4. Butt, H.-J.; Berger, R.; Steffen, W.; Vollmer, D.; Weber, S. A. L., Adaptive wetting - Adaptation in wetting. *Langmuir* **2018**, 34 (38), 11292-11304.
5. Blake, T. D., The physics of moving wetting lines. *J. Colloid Interface Sci.* **2006**, 299 (1), 1-13.
6. Schwartz, A. M.; Tejada, S. B., Studies of dynamic contact angles on solids. *J. Colloid Interface Sci.* **1972**, 38 (2), 359-375.
7. Snoeijer, J. H.; Andreotti, B., Moving contact lines: scales, regimes, and dynamical transitions. *Annu. Rev. Fluid Mech.* **2013**, 45 (1), 269-292.
8. Meuler, A. J.; Smith, J. D.; Varanasi, K. K.; Mabry, J. M.; McKinley, G. H.; Cohen, R. E., Relationships between water wettability and ice adhesion. *Appl. Mater. Interfaces* **2010**, 2 (11), 3100-3110.
9. Ozbay, S.; Yuceel, C.; Erbil, H. Y., Improved Icephobic Properties on Surfaces with a Hydrophilic Lubricating Liquid. *ACS Appl. Mater. Interfaces* **2015**, 7 (39), 22067-77.
10. Chen, D.; Gelenter, M. D.; Hong, M.; Cohen, R. E.; McKinley, G. H., Icephobic surfaces induced by interfacial nonfrozen water. *ACS Appl. Mater. Interfaces* **2017**, 9 (4), 4202-4214.
11. Niemelä-Anttonen, H.; Koivuluoto, H.; Tuominen, M.; Teisala, H.; Juuti, P.; Haapanen, J.; Harra, J.; Stenroos, C.; Lahti, J.; Kuusipalo, J.; Mäkelä, J. M.; Vuoristo, P., Icephobicity of Slippery Liquid Infused Porous Surfaces under Multiple Freeze-Thaw and Ice Accretion-Detachment Cycles. *Adv. Mater. Interfaces* **2018**, 1800828.
12. Juuti, P.; Haapanen, J.; Stenroos, C.; Niemelä-Anttonen, H.; Harra, J.; Koivuluoto, H.; Teisala, H.; Lahti, J.; Tuominen, M.; Kuusipalo, J.; Vuoristo, P.; Mäkelä, J. M., Achieving a slippery, liquid-infused porous surface with anti-icing properties by direct deposition of flame synthesized aerosol nanoparticles on a thermally fragile substrate. *Appl. Phys. Lett.* **2017**, 110 (16), 161603.
13. Kreder, M. J.; Alvarenga, J.; Kim, P.; Aizenberg, J., Design of anti-icing surfaces: smooth, textured or slippery? *Nat. Rev. Mater.* **2016**, 1 (1), 15003.
14. Kim, P.; Wong, T.-S.; Alvarenga, J.; Kreder, M. J.; Adorno-Martinez, W. E.; Aizenberg, J., Liquid-infused nanostructured surfaces with extreme anti-ice and anti-frost performance. *ACS Nano* **2012**, 6 (8), 6569-6577.
15. Momen, G.; Farzaneh, M., Facile approach in the development of icephobic hierarchically textured coatings as corrosion barrier. *Appl. Surf. Sci.* **2014**, 299, 41-46.
16. Janjua, Z. A., The influence of freezing and ambient temperature on the adhesion strength of ice. *Cold Regions Sci. Technol.* **2017**, 140, 14-19.
17. Work, A.; Lian, Y., A critical review of the measurement of ice adhesion to solid substrates. *Prog. Aerospace Sci.* **2018**, 98, 1-26.

18. Launer, P. J.; Arkles, B., *Infrared analysis of organosilicon compounds: Spectra-structure correlations*. Reprinted from *Silicon Compounds: Silanes and Silicones*, 3rd Edition, Gelest, Inc.: Morrisville, PA, 2013.
19. Hanna, R., Infrared absorption spectrum of silicon dioxide. *J. Am. Ceram. Soc.* **1965**, 48 (11), 595-599.
20. Colas, A., Silicones: preparation, properties and performance. *Dow Corning Corporation (Form No. 01-3077-01)*, based on an earlier publication in *Chim. Nouvelle* **1990**, 8, 847-852.
21. Ozbay, S.; Erbil, H. Y., Ice accretion by spraying supercooled droplets is not dependent on wettability and surface free energy of substrates. *Colloids and Surfaces A: Physicochemical and Engineering Aspects* **2016**, 504, 210-218.